

An enzymatic glucose biosensor based on a glassy carbon electrode modified with cylinder-shaped titanium dioxide nanorods

Zhanjun Yang¹ · Youbao Xu¹ · Juan Li¹ · Zhiqin Jian¹ · Suhua Yu¹ · Yongcai Zhang¹ · Xiaoya Hu¹ · Dionysios D. Dionysiou²

Received: 10 February 2015 / Accepted: 8 May 2015 / Published online: 15 May 2015
© Springer-Verlag Wien 2015

Abstract We describe a highly sensitive electrochemical enzymatic glucose biosensor. A glassy carbon electrode was modified with cylinder-shaped titanium dioxide nanorods (TiO₂-NRs) for the immobilization of glucose oxidase. The modified nanorods and the enzyme biosensor were characterized by scanning electron microscopy, X-ray diffraction, Fourier transform infrared spectroscopy, electrochemical impedance spectroscopy and cyclic voltammetry. The glucose oxidase on the TiO₂-NRs displays a high activity and undergoes fast surface-controlled electron transfer. A pair of well-defined quasi-reversible redox peaks was observed at -0.394 and -0.450 V. The TiO₂-NRs provide a good micro-environment to facilitate the direct electron transfer between enzyme and electrode surface. The biosensor has two linear response ranges, viz. from 2.0 to 52 μM, and 0.052 to 2.3 mM. The lower detection limit is 0.5 μM, and the sensitivity is 68.58 mA M⁻¹ cm⁻². The glucose biosensor is selective, well reproducible, and stable. In our perception, the cylindrically shaped TiO₂-NRs provide a promising support for

the immobilization of proteins and pave the way to the development of high-performance biosensors.

Keywords Cylinder-shaped titanium dioxide · Nanorods · Glucose oxidase · Glucose · Biosensor

Introduction

Rapid advance of materials science and nanotechnology has spurred the development of bioelectroanalysis and biosensors [1]. In general, the immobilization of biomolecules on nanostructured interface can remarkably improve the performance of biocatalytic processes and biosensing [2]. Titanium dioxide (TiO₂), a cheap, nontoxic and chemically stable semiconductor with band gap energy of 3.2 eV, has shown considerable importance in various applications, such as pigment, cosmetics, catalysts, photovoltaic materials and sensors [3–7]. It has also been proven that TiO₂ modification on electrode surface can enhance the enzyme catalytic performance for promising biosensing applications due to its excellent properties [8–10]. Previous studies also demonstrated that one-dimensional TiO₂ nanostructures, such as nanorods, nanowires and nanotubes, are superior to their spherical and planar counterparts due to their high surface-to-volume ratio, increased number of delocalized carriers, and improved charge transport afforded by their dimensional anisotropy [3, 4]. Increasing efforts have been dedicated to the synthesis of one-dimensional TiO₂ nanostructures for various applications [11–13]. To the best of our knowledge, cylinder-shaped TiO₂ nanorods (TiO₂-NRs) have not been exploited for applications in the field of electrochemical enzyme biosensing.

The study on direct electron transfer between the functional groups of redox proteins and electrode surface has attracted great interest in both investigating the mechanism of

Electronic supplementary material The online version of this article (doi:10.1007/s00604-015-1519-3) contains supplementary material, which is available to authorized users.

- ✉ Zhanjun Yang
zjyang@yzu.edu.cn
- ✉ Dionysios D. Dionysiou
dionysios.d.dionysiou@uc.edu

¹ Jiangsu Key Laboratory of Environmental Material and Environmental Engineering, College of Chemistry and Chemical Engineering, Yangzhou University, Yangzhou 225002, People's Republic of China

² Environmental Engineering and Science Program, Department of Biomedical, Chemical and Environmental Engineering (DBCEE), University of Cincinnati, Cincinnati, OH 45221-0012, USA

biological redox reactions and developing biosensors and bioelectrocatalytic devices [14–17]. However, direct electron transfer of enzymes at conventional electrodes is hard to realize because the redox centers of biomolecules are usually seated deeply in the cavity of enzyme molecules [18]. Chemically modification of electrodes can provide an electron mediating function to facilitate the direct electron transfer [19–21]. The modification by functional materials on the electrode surface, while retaining high bioactivity of the immobilized enzyme molecules, is of great importance in the field of direct electrochemistry. Over the past decade, various types of nanomaterials, such as noble metal nanoparticles [22–24], carbon nanomaterials [25–28], and semiconductor nanomaterials [10, 29, 30] have been explored to immobilize enzymes for accelerating direct electron transfer of redox enzymes on electrode surfaces.

The determination of blood glucose concentration is of considerable importance for diagnosis and therapy of diabetics [31]. As an ideal model enzyme, glucose oxidase (GOx) has been widely used in fabrication of electrochemical glucose biosensor due to its catalytic ability to oxidize glucose [32–34]. Here, cylinder-shaped TiO₂ nanorods were synthesized by a facile hydrothermal method for the immobilization of GOx. Based on the direct electrochemistry of GOx at an electrode modified with TiO₂-NRs, a highly sensitive electrochemical glucose biosensor was fabricated. The electrochemical behavior of GOx at this electrode was investigated in detail. The results indicate that TiO₂-NRs facilitate the direct electron transfer between the enzyme molecules and electrode surface. Fourier transform infrared spectrum studies confirmed that enzyme molecules immobilized on TiO₂-NRs can retain their original structure and bioactivity. The constructed biosensor shows high sensitivity, wide linear range, and can be successfully applied in reagentless glucose detection at –0.45 V applied potential. The method and knowledge gained from the synthesis and application of TiO₂-NRs open a promising avenue for the development of other biosensors.

Materials and methods

Materials and reagents

GOx (108 U mg⁻¹, from *Aspergillus niger*) was purchased from Amresco (<http://www.amresco-inc.com/>). D-(+)-Glucose and Nafion were bought from Sigma-Aldrich (<http://www.sigma-aldrich.com/>). Titanium tetrachloride, chloroform, and absolute ethanol were bought from Sinopharm Chemical Reagent Co. Ltd (China, <http://sinoreagen.cn.alibaba.com>). A stock solution of D-glucose was prepared and allowed to mutarotate at room temperature for 24 h prior to use. Phosphate buffer was a mixture of 0.1 M Na₂HPO₄ and NaH₂PO₄ and its pH was adjusted with H₃PO₄

or NaOH solutions. All other chemicals and reagents are of analytical grade and were prepared using distilled water.

Apparatus

Electrochemical measurements were carried out on a CHI 852C electrochemical workstation (Co., CHI, Shanghai Chenhua, China). All experiments were performed with a three-electrode system using a glassy carbon electrode (GCE, $D=3$ mm) as the working electrode, a platinum wire as the auxiliary electrode and a saturated calomel electrode (SCE) as reference electrode. The cyclic voltammetry experiments were carried out at a scan rate of 100 mV s⁻¹ in an electrochemical cell filled with 5.0 mL of phosphate buffer. All pH measurements were performed with S-25 digital pH-meter with a glass combination electrode. Electrochemical impedance spectroscopy (EIS) data were recorded on an Autolab/PGSTAT30 (The Netherlands) in 0.1 M KCl solution containing 5 mM K₃[Fe(CN)₆]/K₄[Fe(CN)₆], and the amplitude of the applied sine wave potential was 5 mV. The impedance measurements were performed at a bias potential of 190 mV within the frequency range from 10⁻¹ to 10⁵ Hz. Fourier transform infrared (FTIR) spectra were measured with a Tensor 27 spectrometer (Bruker Co., Germany). X-ray diffraction (XRD) spectra were recorded on D8 Advance X-ray diffractometer (Bruker Co., Germany) at room temperature. Transmission electron micrograph (TEM) was obtained with a Philips Tecnai-12 transmission electron microscope (Holland) at an acceleration voltage of 120 kV. Scanning electron micrographs (SEM) were obtained with a Hitachi S-4800 scanning electron microscope (Japan) at an acceleration voltage of 15 kV.

Preparation of cylinder-shaped TiO₂ nanorods

TiO₂-NRs were synthesized according to our previous method [35]. 19 mL of water were firstly transferred into a 50 mL glass beaker, and the beaker was then kept in an ice-water bath. Titanium tetrachloride (1.8 mL) was slowly added to the water. After the solution was stirred vigorously for 10 min, a white suspension was obtained. Subsequently, 1.8 mL of chloroform was added to the white suspension, stirred for 10 min and then transferred into a Teflon-lined stainless-steel autoclave. The autoclave was placed in an electrothermal oven and maintained at 160 °C for 12 h. The obtained precipitate was collected, washed carefully with distilled water and absolute ethanol until the pH reached about 7.0, and then dried in vacuum at 60 °C for 24 h.

Preparation of the glucose biosensor

The GCE was firstly polished successively with 0.03 and 0.05 μm alumina slurry (Buhler) followed by rinsing

thoroughly with distilled water, and then sonicated in 1:1 nitric acid-water (*v/v*), acetone and distilled water and finally dried in air. One mg of TiO₂-NRs was dispersed in 1.0 mL distilled water. Ten mg of GOx powder was added to the solution of the TiO₂-NRs and stirred gently for 15 min. The resultant suspension was subsequently dropped on the pretreated GCE surface and dried in air. Next, 5.0 μL of 1.0 % Nafion solution was dropped on the surface of GOx/TiO₂-NR/GCE to finally obtain the GOx/TiO₂-NR/Nafion electrode. It was rinsed thoroughly with distilled water to remove loosely adsorbed GOx. When not in use, the glucose biosensor was stored at 4 °C in a refrigerator.

Results and discussion

Characterization of the TiO₂-NRs and the enzyme electrode

The TEM and SEM images of the TiO₂-NRs are shown in Fig. 1a and 1b. The nanorods display an anisotropic and uniform cylinder-like morphology with about 180 nm in length and 20 nm in thickness. Fig. S1 (Supporting information) shows the XRD spectrum of TiO₂-NRs. The product displays only the XRD peaks characteristic of rutile TiO₂ (JCPDS card no. 65–0190), indicating that phase-pure TiO₂ powders have been successfully obtained. After GOx molecules had been immobilized on TiO₂-NRs (Fig. 1c), the SEM image of GOx/TiO₂-NRs exhibited different surface morphology compared with that of single TiO₂-NRs film (Fig. 1b). The uniform aggregates of the loaded enzyme molecules were clearly observed, indicating the successful immobilization of GOx on TiO₂-NRs.

Electrochemical impedance spectroscopy (EIS) is a powerful tool to study the interface properties of the modified electrode. The typical impedance spectrum is described as Nyquist plot, and it consists of a semicircle and a linear parts. The semicircle part is attributed to the electron-transfer limited process at higher frequencies and its diameter represents the electron transfer resistance (R_{ct}), which controls the electron transfer kinetics of the electrode interface. Figure 2a shows the Nyquist plots of various modified electrodes in the frequency

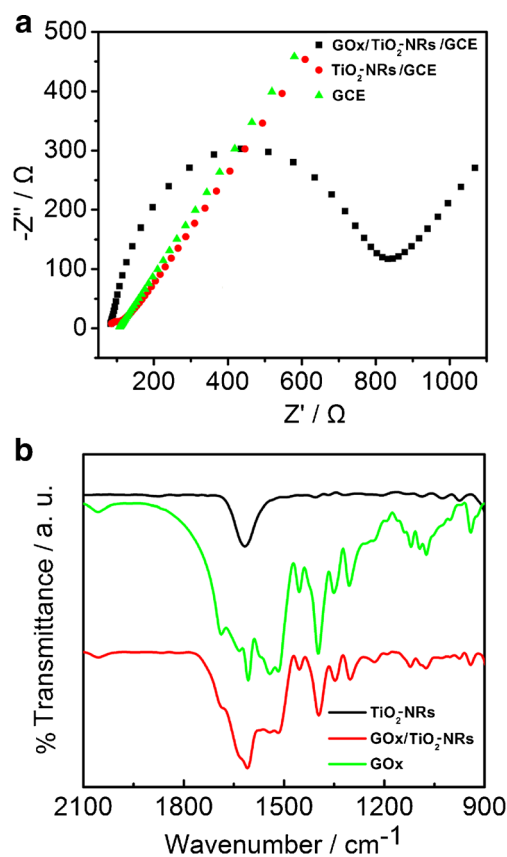
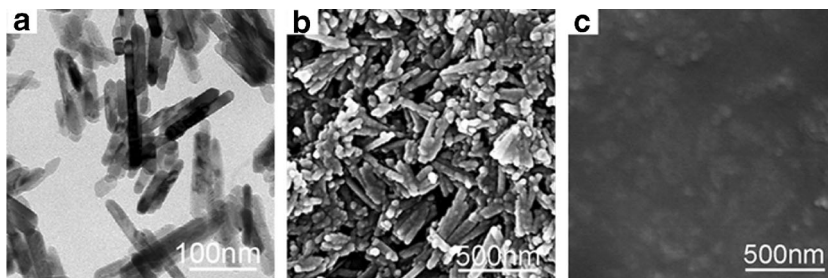


Fig. 2 Nyquist plots of EIS (a) for bare GCE, TiO₂-NR/GCE and GOx/TiO₂-NR/GCE and FTIR spectra of (b) of TiO₂-NRs, GOx and GOx/TiO₂-NRs

range of 10⁻¹ to 10⁵ Hz. The bare GCE displays a very small electron transfer resistance. The R_{ct} of TiO₂-NRs/GCE (61 Ω) is larger than that of the bare GCE, demonstrating that the TiO₂-NR film is formed on the surface of GCE. The results showed after GOx had been trapped in the TiO₂-NR film, the R_{ct} of GOx/TiO₂-NRs significantly increased to 734 Ω. The possible reason is that the formed protein layer on the electrode surface greatly blocked the diffusion of ferricyanide probe toward the electrode surface.

FTIR spectroscopy is a useful tool for studying the structure and conformation of the proteins. Thus the state of the GOx molecules trapped in TiO₂-NRs was examined by FTIR spectroscopy. Figure 2b shows the FTIR spectra of the TiO₂-NRs, native GOx and GOx/TiO₂-NRs. An absorption band at

Fig. 1 TEM image of TiO₂-NRs (a), SEM images of TiO₂-NRs (b) and GOx immobilized TiO₂-NRs (c)



1620 cm^{-1} of TiO_2 -NRs is the characteristic peak of $-\text{OH}$ on the surface of TiO_2 , which results from the bending vibration of water. Two characteristic peaks at 1605 and 1537 cm^{-1} from the FTIR spectrum of native GOx were observed, which are ascribed to amide I and II bands of the enzyme. The FTIR spectrum of GOx/ TiO_2 -NRs also shows two characteristic absorption peaks at 1610 (amide I band) and 1542 (amide II band) cm^{-1} , indicating that GOx molecules were immobilized on the TiO_2 -NR film with their native structure. Minor shifts for amide I and II bands of the native GOx and loaded GOx in TiO_2 -NRs may result from the molecular interaction between enzyme and TiO_2 film.

Direct electrochemistry of the GOx/ TiO_2 -NR/Nafion/GCE

The cyclic voltammograms of different modified GCEs in 0.1 M N_2 -saturated phosphate buffer at a scan rate of 100 mV s^{-1} are shown in Fig. 3. No redox peaks were observed from Nafion/GCE (curve a) and TiO_2 -NR/Nafion/GCE (curve b). However, the TiO_2 -NR/Nafion/GCE shows higher background current compared with that of Nafion/GCE, which may be attributed to the larger surface area of TiO_2 -NRs [27]. The GOx/Nafion/GCE (curve c) exhibits a pair of weak redox peaks, while the GOx/ TiO_2 -NR/Nafion/GCE shows a pair of more distinct and better-defined redox peaks at -0.394 and -0.450 V (curve d), indicating that TiO_2 -NRs can enhance the direct electron transfer of GOx molecules. The reduction peak current of the GOx/ TiO_2 -NR/Nafion/GCE is 1.1 times larger than that of GOx/Nafion/GCE, which may be due to the larger specific surface area [29]. The peak potential separation is 56 mV , which is much smaller than that of 80 mV for the GOx/graphene-chitosan modified GCE [27], indicating a faster direct electron transfer between the electroactive center of GOx and GCE surface.

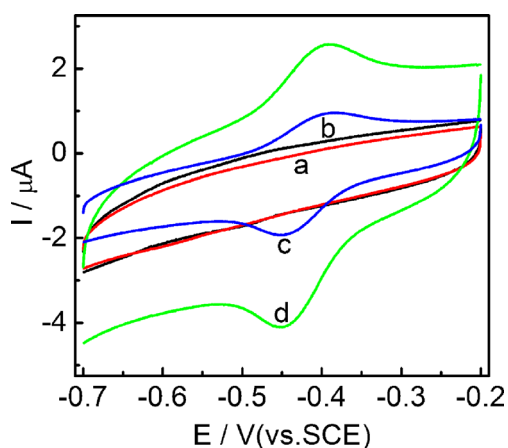


Fig. 3 Cyclic voltammograms of various electrodes: Nafion/GCE (a), TiO_2 -NR/Nafion/GCE (b), GOx/Nafion/GCE (c), and GOx/ TiO_2 -NR/Nafion/GCE (d) in $0.1\text{ M pH } 7.0\text{ N}_2$ -saturated phosphate buffer at a scan rate of 100 mV s^{-1}

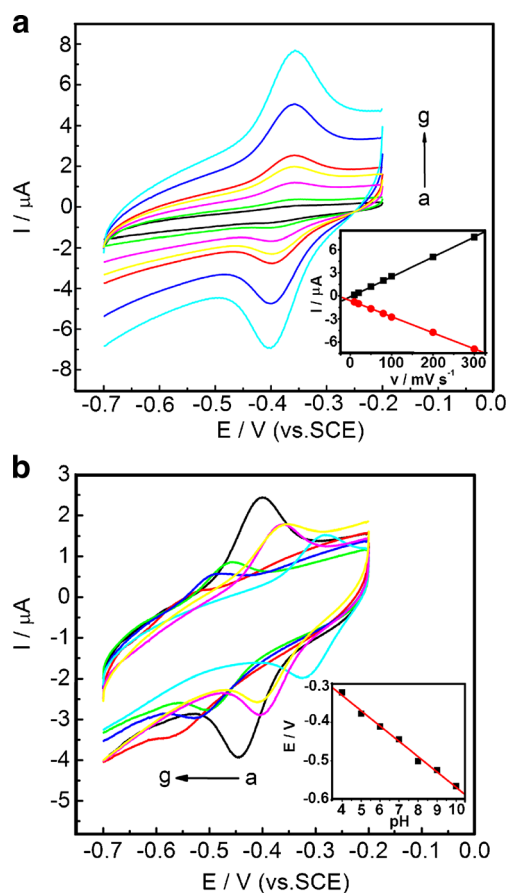


Fig. 4 a Cyclic voltammograms of the GOx/ TiO_2 -NR/Nafion/GCE in N_2 -saturated $0.1\text{ M pH } 7.0$ phosphate buffer at $10, 20, 50, 80, 100, 150,$ and 200 mV s^{-1} (a–g), inset: plots of anodic and cathodic peak currents vs. scan rates; b Cyclic voltammograms of the GOx/ TiO_2 -NR/Nafion/GCE in N_2 -saturated 0.1 M phosphate buffer with different pH values of (a–g) $4.0, 5.0, 6.0, 7.0, 8.0, 9.0$ and 10.0 at a scan rate of 100 mV s^{-1} , inset: plot of formal potentials vs. pH

Figure 4a shows the effect of the scan rate on the redox peaks current at the GOx/ TiO_2 -NR/Nafion/GCE. It can be seen that the anodic current (I_{pa}) and cathodic peak current (I_{pc}) linearly increase with the increasing scan rate from 10 to 400 mV s^{-1} (inset of Fig. 4a). The I_{pa}/I_{pc} ratio is approximately equal to 1, indicating a quasi-reversible surface-controlled process. The surface coverage (Γ^*) of the enzyme molecules on the surface of the TiO_2 -NR/Nafion modified electrode can be obtained according to the equation $\Gamma^* = Q/nFA$ (where Q is the charge consumed in the reaction, n the number of electrons transferred, F the Farady constant, and A the electrode area). The Γ^* of the GOx molecules on the TiO_2 -NR/Nafion/GCE was calculated to be $1.22 \times 10^{-10}\text{ mol cm}^{-2}$, which is larger than those of $1.60 \times 10^{-11}\text{ mol cm}^{-2}$ at GOx/SnS₂/Nafion/GCE [30], $9.8 \times 10^{-12}\text{ mol cm}^{-2}$ at GOx/Au nanoparticles/carbon paste electrode [22], and $7.82 \times 10^{-12}\text{ mol cm}^{-2}$ at GOx/Au-dihexadecyl phosphate modified electrode [36]. The apparent electron transfer rate constant (k_s) of the present biosensor was calculated to be 3.24 s^{-1}

according to Laviron's equation. The obtained ks value is larger than those of 1.56 s^{-1} for boron-doped carbon nanotubes [37], 1.96 s^{-1} for Nafion-graphene modified gold disk electrode [38], and 2.83 s^{-1} at graphene-chitosan modified GCE [27], indicating that TiO_2 -NRs facilitate the fast electron transfer between redox-active site of enzyme and the surface of electrode.

Figure 4b shows the influence of solution pH value on the electrochemical behavior of the GOx/ TiO_2 -NR/Nafion/GCE. Both the cathodic and anodic peak potentials shift negatively with increasing solution pH. The redox potentials of the GOx/ TiO_2 -NRs/Nafion/GCE change linearly as a function of the solution pH from 4.0 to 10.0 with a slope of -49.6 mV pH^{-1} (inset of Fig. 4b). This slope is close to the theoretical value of -58.6 mV pH^{-1} reported previously [26], indicating the same proton and the same electron participating in the electron transfer process.

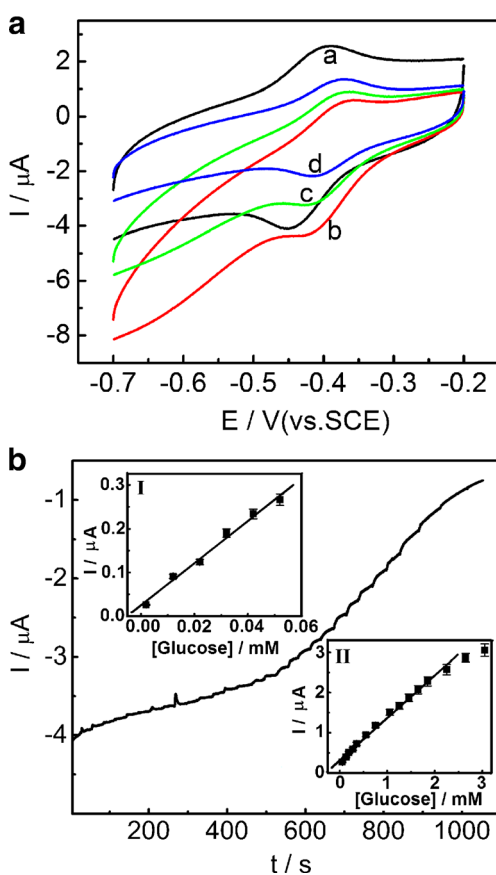


Fig. 5 a Cyclic voltammograms of the GOx/ TiO_2 -NRs/Nafion/GCE in 0.1 M pH 7.0 N_2 -saturated (a), air-saturated (b), and air-saturated phosphate buffer including 0.5 and 1.0 mM glucose (c and d) at a scan rate of 100 mV s^{-1} ; b typical steady-state response of the GOx/ TiO_2 -NRs/Nafion/GCE on successive addition of glucose into 0.1 M pH 7.0 air-saturated phosphate buffer at the applied potential of -0.45 V , insets: calibration curve for glucose

Performance of the glucose biosensor

Figure 5a shows the cyclic voltammograms of the GOx/ TiO_2 -NRs/Nafion/GCE in nitrogen- and air-saturated pH 7.0 phosphate buffer in the absence and presence of glucose. The GOx/ TiO_2 -NRs/Nafion/GCE shows a pair of distinct and well-defined redox peaks in nitrogen-saturated phosphate buffer. In air-saturated phosphate buffer, a great increase in reduction peak current and a simultaneous decrease in oxidation current were clearly observed at this GCE. Upon addition of glucose to air-saturated phosphate buffer, the reduction peak current decreases correspondingly.

Figure 5b displays the amperometric response curve for the GOx/ TiO_2 -NR/Nafion/GCE on successive injection of glucose to the air-saturated stirring pH 7.0 phosphate buffer at -0.45 V applied potential. The GCE achieves 95 % of the steady-state current within only 7 s. The current response increases linearly with the increase of glucose concentration from 2.0 to 52 μM and 0.052 to 2.3 mM with a high sensitivity of $68.58 \text{ mA M}^{-1} \text{ cm}^{-2}$. The detection limit is 0.5 μM at a signal-to-noise ratio of 3. The high sensitivity of the biosensor may be because cylinder-shaped TiO_2 nanorods can provide a good microenvironment for retaining high bioactivity of loaded enzyme and enhancing the direct electron transfer. The present glucose biosensor was compared with other glucose biosensors reported in recent literature, which are listed in Table 1. Compared with other types of enzyme electrodes, the present GCE shows obvious advantages such as much higher sensitivity and lower detection limit.

Reproducibility and stability of the glucose biosensor

The reproducibility of the biosensor was investigated by measuring 0.1 mM glucose solution for 10 times at the same enzyme electrode. The relative standard deviation (RSD) was 2.5 %, suggesting good repeatability. After 30 times successive detections, the response was 96 % of the initial response, demonstrating acceptable sensor durability. The reproducibility of the enzyme electrode was also examined by testing 0.1 mM glucose solution with 5 different enzyme electrodes. The RSD was 2.7 %, indicating good fabrication reproducibility. The enzyme electrode was stored at $4 \text{ }^\circ\text{C}$ when not in use. After storage for 25 days, the biosensor was able to retain 97 % of its initial current response, demonstrating that TiO_2 -NRs provide a favorable microenvironment to retain the bioactivity of the loaded enzyme molecules.

Selectivity studies

The effect of possible interfering species on the quantitative detection of glucose was studied using 0.1 mM ascorbic acid (AA), 0.1 mM uric acid (UA) and 0.1 mM dopamine (DA) at an applied potential of -0.45 V . As shown in Fig. 6, a clear

Table 1 Comparison of analytical performance between the GOx/TiO₂-NRs/Nafion/GCE and other enzyme electrodes

Electrode	Applied potential (V)	Sensitivity (mA M ⁻¹ cm ⁻²)	Detection limit (mM)	Linear range (mM)	Reference
GOx/TiO ₂ nanofiber/Pt electrode	+0.60	9.25	0.01	0.01–6.98	[39]
GOx/TiO ₂ -graphene/GCE	-0.60	6.2	–	0.0–8.0	[40]
^a RGO/Ag/GOx/GCE	-0.49	3.84	0.16	0.5–12.5	[41]
GOx/ ^b TPSP-ZnO/Nafion/GCE	-0.50	–	0.01	0.05–8.2	[29]
GOx/ ^c CNx-MWNTs/GCE	-0.50	13.0	0.01	0.02–1.02	[27]
GOx/SnS ₂ /Nafion/GCE	-0.45	7.6	0.01	0.025–1.1	[30]
GOx/Pt/ ^d FCNA/GCE	-0.08	6.0	0.3	0.5–8.0	[42]
GOx/ TiO ₂ -NRs/Nafion/GCE	-0.45	68.58	0.0005	0.002–0.052 0.052–2.3	This work

^a RGO: reduced graphene oxide

^b TPSP: tetragonal pyramid-shaped porous

^c CNx-MWNTs: nitrogen-doped carbon nanotubes

^d FCNA: flower-like carbon nanosheet aggregation

current response appears upon the addition of 0.2 mM glucose to pH 7.0 phosphate buffer. On the other hand, successive injections of AA, UA and DA in the solution, leads to no obvious increase of the current. When 0.2 mM glucose was added in the system again, the amperometric response was very close to the value detected in the absence of the interferents, demonstrating the excellent selectivity of the constructed glucose biosensor toward glucose.

Determination of glucose in human serum sample

To evaluate the practicality of the glucose biosensor, glucose in human serum samples was determined by the present enzyme electrode. The human serum samples were received from Northern Jiangsu People's Hospital without any sample pretreatment except a dilution step. The glucose concentration was measured to be 4.42 mM, which is close to the value of

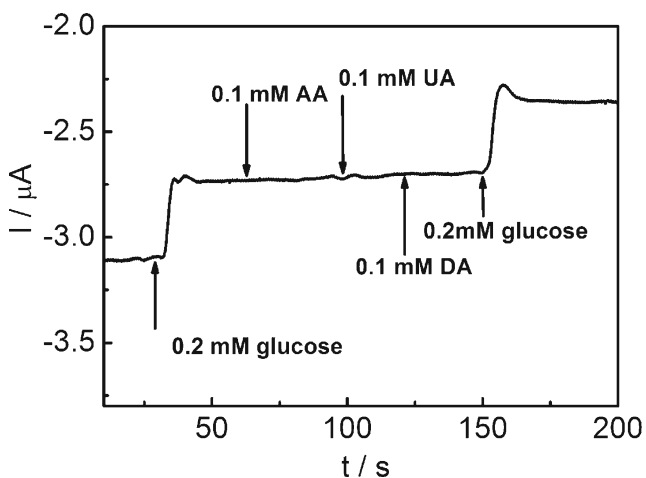


Fig. 6 Amperometric response of the GOx/TiO₂-NRs/Nafion/GCE to 0.2 mM glucose, 0.1 mM AA, 0.1 mM UA and 0.1 mM DA in pH 7.0 phosphate buffer at -0.45 V applied potential

4.53 mM measured by enzyme catalytic spectrophotometry. The recovery test was carried out by assaying 0.1, 0.2 and 0.3 mM glucose added in the human serum samples. The recovery results were 106 % (RSD=3.2 %), 105 % with (RSD=2.7 %), and 103 % (RSD =1.3 %) for five measurements, validating that the glucose biosensor can be used in the detection of human serum samples.

Conclusions

A highly sensitive electrochemical glucose biosensor was developed by the immobilization of GOx onto TiO₂-NRs. The direct electron transfer of GOx was successfully achieved at TiO₂-NRs modified glassy carbon electrode. The immobilized GOx on the TiO₂-NR matrix retained high bioactivity. The prepared TiO₂-NRs provided a good microenvironment for loaded enzyme molecules and enhanced the electron transfer between GOx and electrode surface. The fabricated glucose biosensor demonstrated high sensitivity, low detection limit, wide linear range, excellent selectivity, good reproducibility, and acceptable stability. The satisfactory results for the detection of human serum samples demonstrated potential for practical application of the present glucose biosensor. This research provides a potential sensing platform for the development of sensitive and selective electrochemical biosensors.

Acknowledgments This work was financially supported by National Natural Science Foundation of China (21475116, 21275124), The Priority Academic Program Development of Jiangsu Higher Education Institution (PAPD), University Natural Science Foundation of Jiangsu Province (13KJB150039) and the Open Research Fund of State Key Laboratory of Analytical Chemistry for Life Science (SKLACLS1410). Also, many thanks to The Testing Center of Yangzhou University for all the characterizations.

References

1. Wang Y, Shao YY, Matson DW, Li JH, Lin YH (2010) Nitrogen-doped graphene and its application in electrochemical biosensing. *ACS Nano* 4:1790
2. Dong SY, Li N, Suo GC, Huang TL (2013) Inorganic/organic doped carbon aerogels as biosensing materials for the detection of hydrogen peroxide. *Anal Chem* 85:11739
3. Koo B, Park J, Kim Y, Choi SH, Sung YE, Hyeon T (2006) Simultaneous phase- and size-controlled synthesis of TiO₂ nanorods via non-hydrolytic sol-gel reaction of syringe pump delivered precursors. *J Phys Chem B* 110:24318
4. Wang Z, Xia D, Chen G (2008) The effects of different acids on the preparation of TiO₂ nanostructure in liquid media at low temperature. *Mater Chem Phys* 111:313
5. Liang HC, Li XZ (2009) Effects of structure of anodic TiO₂ nanotube arrays on photocatalytic activity for the degradation of 2,3-dichlorophenol in aqueous solution. *J Hazard Mater* 162:1415
6. Shi XH, Gu W, Li BY, Chen NN, Zhao K, Xian YZ (2014) Enzymatic biosensors based on the use of metal oxide nanoparticles. *Microchim Acta* 181:1
7. Tu WW, Lei JP, Ding L, Ju HX (2009) Sandwich nanohybrid of single-walled carbon nanohorns-TiO₂-porphyrin for electrocatalysis and amperometric biosensing towards chloramphenicol. *Chem Commun* 28:4227
8. Lu JS, Li HN, Cui DM, Zhang YJ, Liu SQ (2014) Enhanced enzymatic reactivity for electrochemically driven drug metabolism by confining cytochrome P450 enzyme in TiO₂ nanotube arrays. *Anal Chem* 86:8003
9. Topoglidis E, Campbell CJ, Cass AEG, Durrant JR (2001) Factors that affect protein adsorption on nanostructured titania films. A novel spectroelectrochemical application to sensing. *Langmuir* 17:7899
10. Yu JH, Liu SQ, Ju HX (2003) Glucose sensor for flow injection analysis of serum glucose based on immobilization of glucose oxidase in titania sol-gel membrane. *Biosens Bioelectron* 19:401
11. Tian G, Fu H, Jing L, Xin B, Pan K (2008) Preparation and characterization of stable biphasic TiO₂ photocatalyst with high crystallinity, large surface area, and enhanced photoactivity. *J Phys Chem C* 112:3083
12. Attar AS, Ghamsari MS, Hajiesmaeilbaigi F, Mirdamdi S, Katagiri K, Koumoto K (2009) Sol-gel template synthesis and characterization of aligned anatase-TiO₂ nanorod arrays with different diameter. *Mater Chem Phys* 113:856
13. Chung YA, Lee CY, Peng CW, Chiu HT (2006) Reactive template assisted growth of one-dimensional nanostructures of titanium dioxide. *Mater Chem Phys* 100:380
14. Wei JJ, Liu HY, Dick AR, Yamamoto H, He YF, Waldeck DH (2002) Direct wiring of cytochrome c's heme unit to an electrode: electrochemical studies. *J Am Chem Soc* 124:9591
15. Xiao Y, Patolsky F, Katz E, Hainfeld JF, Willner I (2003) "Plugging into enzymes": nanowiring of redox enzymes by a gold nanoparticle. *Science* 299:1877
16. Beissenhirtz MK, Scheller FW, Stocklein WFM, Kurth DG, Mhwald H, Lisdat F (2004) Electroactive cytochrome c multilayers within a polyelectrolyte assembly. *Angew Chem Int Ed* 43:4357
17. Mu C, Zhao Q, Xu D, Zhuang Q, Shao Y (2007) Silicon nanotube array/gold electrode for direct electrochemistry of cytochrome c. *J Phys Chem B* 111:1491
18. Meng L, Jin J, Yang GX, Lu TH, Zhang H, Cai CX (2009) Nonenzymatic electrochemical detection of glucose based on palladium-single-walled carbon nanotube hybrid nanostructures. *Anal Chem* 81:7271
19. Gooding JJ, Wibowo R, Liu JQ, Yang WR, Losic D, Orbons S, Mearns FJ, Shapter JG, Hibbert DB (2003) Protein electrochemistry using aligned carbon nanotube arrays. *J Am Chem Soc* 125:9006
20. Lee S, Ringstrand BS, Stone DA, Firestone MA (2012) Electrochemical activity of glucose oxidase on a poly(ionic liquid)-Au nanoparticle composite. *ACS Appl Mater Interfaces* 4:2311
21. Liu AH, Wei MD, Honma I, Zhou HS (2005) Direct electrochemistry of myoglobin in titanate nanotubes film. *Anal Chem* 77:8068
22. Liu SQ, Ju HX (2003) Reagentless glucose biosensor based on direct electron transfer of glucose oxidase immobilized on colloidal gold modified carbon paste electrode. *Biosens Bioelectron* 19:177
23. Jia F, Shan CS, Li FH, Niu L (2008) Carbon nanotube/gold nanoparticles/polyethylenimine-functionalized ionic liquid thin film composites for glucose biosensing. *Biosens Bioelectron* 24:945
24. Pingarron JM, Yanez-Sedeno P, Gonzalez-Cortes A (2008) Gold nanoparticle-based electrochemical biosensors. *Electrochim Acta* 53:5848
25. Azamian BR, Davis JJ, Coleman KS, Bagshaw CB, Green MLH (2002) Bioelectrochemical single-walled carbon nanotubes. *J Am Chem Soc* 124:12664
26. Deng SY, Jian GQ, Lei JP, Hu Z, Ju HX (2009) A glucose biosensor based on direct electrochemistry of glucose oxidase immobilized on nitrogen-doped carbon nanotubes. *Biosens Bioelectron* 25:373
27. Kang XH, Wang J, Wu H, Aksay IA, Liu J, Lin YH (2009) Glucose oxidase-graphene-chitosan modified electrode for direct electrochemistry and glucose sensing. *Biosens Bioelectron* 25:901
28. Shan CS, Yang HF, Han DX, Zhang Q, Ivaska A, Niu L (2010) Electrochemical determination of NADH and ethanol based on ionic liquid-functionalized graphene. *Biosens Bioelectron* 25:1070
29. Dai ZH, Shao GJ, Hong JM, Bao JC, Shen J (2009) Immobilization and direct electrochemistry of glucose oxidase on a tetragonal pyramid-shaped porous ZnO nanostructure for a glucose biosensor. *Biosens Bioelectron* 24:1286
30. Yang ZJ, Ren YY, Zhang YC, Li J, Li HB, Huang XC, Hu XY, Xu Q (2011) Nanoflake-like SnS₂ matrix for glucose biosensing based on direct electrochemistry of glucose oxidase. *Biosens Bioelectron* 26:4337
31. Steiner MS, Duerkop A, Wolfbeis OS (2011) Optical methods for sensing glucose. *Chem Soc Rev* 40:4805
32. Vamvaki V, Tsagaraki K, Chaniotakis N (2006) Carbon nanofiber-based glucose biosensor. *Anal Chem* 78:5538
33. Xu XA, Jiang SJ, Hu Z, Liu SQ (2010) Nitrogen-doped carbon nanotubes: high electrocatalytic activity toward the oxidation of hydrogen peroxide and its application for biosensing. *ACS Nano* 4:4292
34. Yu JC, Zhang YJ, Liu SQ (2014) Enzymatic reactivity of glucose oxidase confined in nanochannels. *Biosens Bioelectron* 55:307
35. Yang ZJ, Jian ZQ, Chen X, Li J, Qin PY, Zhao J, Jiao XA, Hu XY (2015) Electrochemical impedance immunosensor for subpicogram level detection of bovine interferon gamma based on cylinder-shaped TiO₂ nanorods. *Biosens Bioelectron* 63:190
36. Wu YH, Hu SS (2007) Direct electrochemistry of glucose oxidase in a colloid Au-dihexadecylphosphate composite film and its application to develop a glucose biosensor. *Bioelectrochemistry* 70:335
37. Deng CY, Chen JH, Chen XL, Xiao CH, Nie LH, Yao SZ (2008) Direct electrochemistry of glucose oxidase and biosensing for glucose based on boron-doped carbon nanotubes modified electrode. *Biosens Bioelectron* 23:1272
38. Hui JN, Cui JW, Xu GQ, Adeloju SB, Wu YC (2013) Direct electrochemistry of glucose oxidase based on Nafion-graphene-GOD modified gold electrode and application to glucose detection. *Mater Lett* 108:88
39. Tang H, Yan F, Tai QD, Chan HLW (2010) The improvement of glucose bioelectrocatalytic properties of platinum electrodes

- modified with electrospun TiO₂ nanofibers. *Biosens Bioelectron* 25:1646
40. Jang HD, Kim SK, Chang H, Roh KM, Choi JW, Huang JX (2012) A glucose biosensor based on TiO₂-Graphene composite. *Biosens Bioelectron* 38:184
41. Palanisamy S, Karupiah C, Chen SM (2014) Direct electrochemistry and electrocatalysis of glucose oxidase immobilized on reduced graphene oxide and silver nanoparticles nanocomposite modified electrode. *Colloids Surface B* 114:164
42. Tang S, Wang XZ, Lei JP, Hu Z, Deng SY, Ju HX (2010) Pt-dispersed flower-like carbon nanosheet aggregation for low-overpotential electrochemical biosensing. *Biosens Bioelectron* 26:432